Enhanced J c and improved grain-boundary properties in Ag-doped YBa 2 Cu 3 O 7−δ films

P. Selvam, E. W. Seibt, D. Kumar, R. Pinto, and P. R. Apte

Citation: Applied Physics Letters **71**, 137 (1997); doi: 10.1063/1.119452
View online: http://dx.doi.org/10.1063/1.119452
View Table of Contents: http://scitation.aip.org/content/aip/journal/apl/71/1?ver=pdfcov
Published by the AIP Publishing

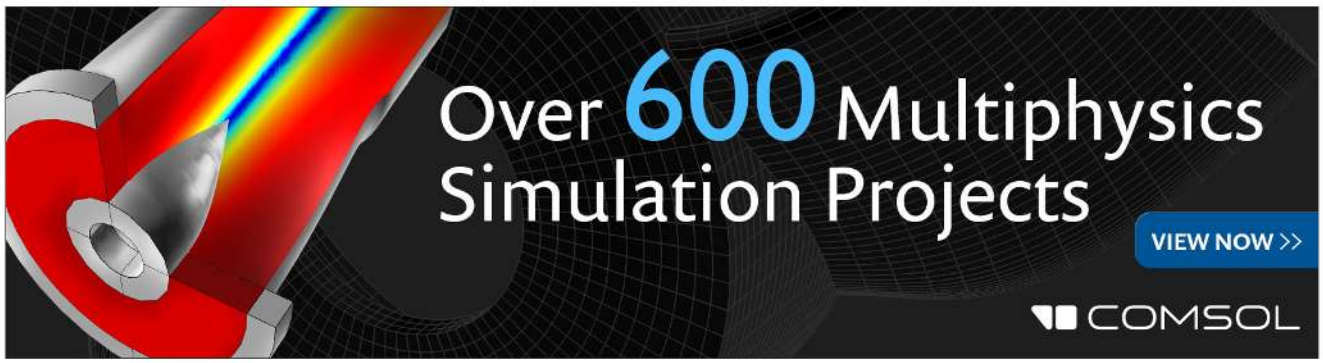

Enhanced J_c and improved grain-boundary properties in Ag-doped $YBa_2Cu_3O_{7-\delta}$ films

P. Selvam[a)]
Department of Chemistry, Indian Institute of Technology, Powai, Bombay 400 076, India

E. W. Seibt
Institut für Technische Physik, Forschungszentrum Karlsruhe, Postfach 3640, D-76021 Karlsruhe, Germany

D. Kumar, R. Pinto, and P. R. Apte
Tata Institute of Fundamental Research, Colaba, Bombay 400 005, India

(Received 30 May 1996; accepted for publication 2 April 1997)

A large increase ($\sim 8\times$) in critical current density, J_c, was achieved for *in situ* laser ablated $YBa_2Cu_3O_{7-\delta}$–Ag films. High-resolution Auger electron spectroscopic investigation indicates that the Ag-doped films are stoichiometric with a relatively low grain-boundary extension (8 nm) in contrast to undoped $YBa_2Cu_3O_{7-\delta}$ films (32 nm). Further analysis suggests that the doped film contains a much lower silver content (<0.15 wt %) than in the target material (5 wt %). These observations are in excellent agreement with the temperature dependence of J_c, the room-temperature resistivity, and the surface resistance results. Thus, J_c enhancement in Ag-doped films can be attributed to their superior properties, viz., improved microstructure characteristics and the reduced resistive grain boundaries. © *1997 American Institute of Physics.* [S0003-6951(97)03022-2]

Of the numerous studies on chemical modifications in superconducting $YBa_2Cu_3O_{7-\delta}$, the addition of silver is by far the most extensively studied, due to its ability to enhance performance.[1–12] Although the *intragranular* critical current densities, J_c approach the intrinsic values, the *intergranular* weak links still limit the current carrying capacity.[2,5,13–18] Microstructure and granularity problems are the key issues of great interest. Here, we report high-resolution Auger electron spectroscopic (HRAES) results, and address the nature and thickness of the grain boundaries in laser ablated $YBa_2Cu_3O_{7-\delta}$ thin films.

Undoped and Ag-doped $YBa_2Cu_3O_{7-\delta}$ films, 1000–4000 Å were grown *in situ* on $LaAlO_3$ (100) substrates at 700 °C by a pulsed-laser ablation technique (248 nm KrF source; 3 J cm^{-2} fluence on the target; 200 mTorr O_2 pressure), respectively, from $YBa_2Cu_3O_{7-\delta}$ and $YBa_2Cu_3O_{7-\delta}$ containing 5.0 wt % (2.17 at. %) Ag.[8,9] The films were characterized by x-ray diffraction [(XRD); JEOL-8030] using 0.02° step angle and 1 s count times. The composition of the films were analyzed by an energy dispersive x-ray [(EDX); Kevex-8000] microanalyzer. The superconducting transition temperature, T_c, was measured resistively using the standard four-probe method. J_c was measured using patterned 10 μm wide and 1.5 mm long microbridges with evaporated Ag contacts. A voltage criterion of 1 μV/mm was employed. Scanning electron microscopy [(SEM); JEOL-840] studies were carried out on films partially etched with 0.5% acetic acid to delineate the grains.

HRAES measurements were carried out using a PHI multiprobe 600 (Perkin-Elmer) equipped with scanning Auger microscopy (SAM), SEM, and EDX facilities. The SEM mode is used to select areas of particular interest and, subsequently, Auger analysis was made in the specified regions (electron beams: 10 keV, 100 nA with a beam diameter of ~ 400 nm, incidence angle 45°; argon ion sputtering: 6 keV, 10 nA, incidence angle 41°; sputter rate ~ 7 nm min^{-1}). As the use of standard sensitivity factors (SSF) (Ref. 19) leads to erroneous results[20] in the quantification of AES data, a calibration is performed on the stoichiometrically known $YBa_2Cu_3O_{7-\delta}$ standard to determine the relative sensitivity factors (RSF).[21] Table I summarizes the essential Auger parameters. In order to study the grain-boundary weak-link behavior, we have used transmission-type two-port capacitive gap-coupled X-band microstrip resonators of (10 mm$\times$10 mm) undoped and Ag-doped films.[22] The microwave measurements were carried out at X-band frequencies (8–12 GHz) using a HP8757C scalar network analyzer with associated reflectometry setup. The microwave power source used was a HP83620A synthesized sweeper and the input power level applied was in the range -15 to $+13$ dBm. A closed cycle He cryocooler was used for the low-temperature measurements.

XRD results indicate that the films are highly crystalline, single-phase and c-axis oriented. Ag-doped films exhibit better crystallinity; full width at half-maximum (FWHM) of (005) reflection is considerably narrower (0.2°) than the undoped films (0.3°). It is, however, to be noted here that the

TABLE I. Auger quantification data for $YBa_2Cu_3O_{7-\delta}$.

Element	Elemental composition (at. %) Single crystal[a]	Theoretical	Auger level	Auger energy (eV)	RSF[b] (at 10 keV)	SSF[c] (at 10 keV)
Y	7.7	7.69	LMM	1746	0.100	0.038
Ba	15.4	15.35	MNN	584/600	0.125	0.082
Cu	23.1	23.08	LMM	920	0.105	0.215
O	53.8	53.85	KLL	510	0.170	0.350

[a]From XRD refinement.
[b]For stoichiometric $YBa_2Cu_3O_{7-\delta}$ single crystal (column 2).
[c]For pure elements related to silver metal (Ref. 19).

[a)]Electronic mail: selvam@ether.chem.iitb.ernet.in

TABLE II. Some properties of laser ablated $YBa_2Cu_3O_{7-\delta}$ films.

Sample	Silver content (wt. %)		Elemental composition (at. %)[a]				$T_{c(0)}$ (K)	J_c at 77 K and $B=0$ T (A cm^{-2})	$\rho_{300\,K}$ ($\mu\Omega$ cm)	Grain size (μm)	$\rho_{300\,K}/\rho_{100\,K}$	$\sqrt{J_c}/T_c-T$	d_{gb} (nm) (half-width)	Lattice constant, ''c'' (nm)	R_s at 77 K and 10 GHz ($\mu\Omega$)
	Target	Film	Y	Ba	Cu	O									
Undoped	0	0	7.72	15.42	19.58	53.95	89	1.1×10^6	250	0.3–0.5	3.0	60	32	1.173	400
Ag-doped	5.0	<0.15	7.70	15.39	23.07	53.75	90	9.0×10^6	150	1.0	2.6	200	8	1.170	190

[a]From AES data, calculated using RSF values (see Table I); ideal composition: Y 7.69, Ba 15.39, Cu 23.08, and O 53.85.

films grown at 650 °C show considerably larger FWHM, viz., 0.4 and 0.65, respectively, for the Ag-doped and undoped ones. Nevertheless, it follows the same trend of the films under investigation. SEM of partially etched films indicate square plateletlike morphology.[8,9] The latter, however, shows significant grain growth, uniform grain-size distribution and the alignment of the grains. The enhanced grain sizes and the improved grain alignment decreases the number of grain boundaries over a specified area, as well as the basal plane tilted angle grain boundaries. This results in reduced contact resistance in the intergranular regions, and as a result, the normal-state resistivity is considerably reduced. On the contrary, the undoped films display a broad distribution of the grain sizes, and that the grains are much smaller with larger tilt angles. The increase of misorientation across the boundaries leads to an effective larger grain-boundary area, which in turn behaves as a resistive-type grain boundary and, hence, lower transport J_c. This is in good agreement with the earlier reports[14–18] where the J_c of the basal plane grain boundaries is found to be decreasing with increasing misorientation across the boundary. That is, when the tilt angles of the grain boundaries are more than 20°, they behave as a weak link. Table II summarizes some of the important properties of $YBa_2Cu_3O_{7-\delta}$ films.

Shown in Fig. 1 are the Auger elemental concentration depth profiles of $YBa_2Cu_3O_{7-\delta}$ films. The initial fall or rise in the concentrations are often taken to reflect grain surface compositions.[13,14,23,24] They, however, attain a steady state after short sputtering. The residual concentrations after long sputtering ($\sim$12–14 min) are the composition at the interface of the film and the substrate. While the depth profiles of the Ag film show nearly an ideal stoichiometric composition, a reduction in the copper concentration ($\sim$3–5 at. %) is noted for certain undoped films, suggesting possible off-stoichiometry. Careful analysis of Auger results indicates that silver is located mainly in agglomerates on the film surface and only a small part, <0.15 wt % (0.5 at. %), is present in the film. Surface resistance,[8] R_s, SAM,[25] and inductively coupled plasma atomic emission spectroscopy (ICPAES)[26] studies support this observation.

It is now well established that the high T_c cuprate superconductors are granular, as a consequence, they exhibit characteristic junction properties.[15,16] The Auger depth profiles (Fig. 1) are consistent with these findings and clearly indicate that the near-surface elemental composition pattern, in both cases, is completely different compared to the interior of the grain. Interestingly, a considerable decrease of the grain-boundary width, marked by arrows in Fig. 1, is noticed for the Ag-doped film. The observation is in agreement with the temperature dependence of J_c (Fig. 2), where the large slope in the Ag-doped film indicates the narrowing the the grain boundaries. Near T_c, both the grain and grain-boundary J_c display a temperature dependence such that $J_c\alpha(T_c-T)^n$. The exponent is found to vary (1.5–3.5) with thicknesses of the film, as well as the grain boundary,[27,28] but it takes an average value of 2 for $YBa_2Cu_3O_{7-\delta}$.[29] Thus, the variation of J_c with T for a S–N–S junction can be expressed as[30,31]

$$J_c(T)\propto(T_c-T)^2e^{-d_{gb}/\xi_n(T)} \tag{1}$$

or

$$\sqrt{J_c(T)}\propto(T_c-T)e^{-d_{gb}/2\xi_n(T)}, \tag{2}$$

where ''d_{gb}'' is the thickness of the grain-boundary layer and ξ_n is the normal-metal (i.e., grain-boundary) coherence length. A linear dependence, close to T_c, of $\sqrt{J_c(T)}$ versus (T_c-T) reveals that the grain boundaries are metallic, implying characteristic S–N–S behavior.[8,9] However, higher

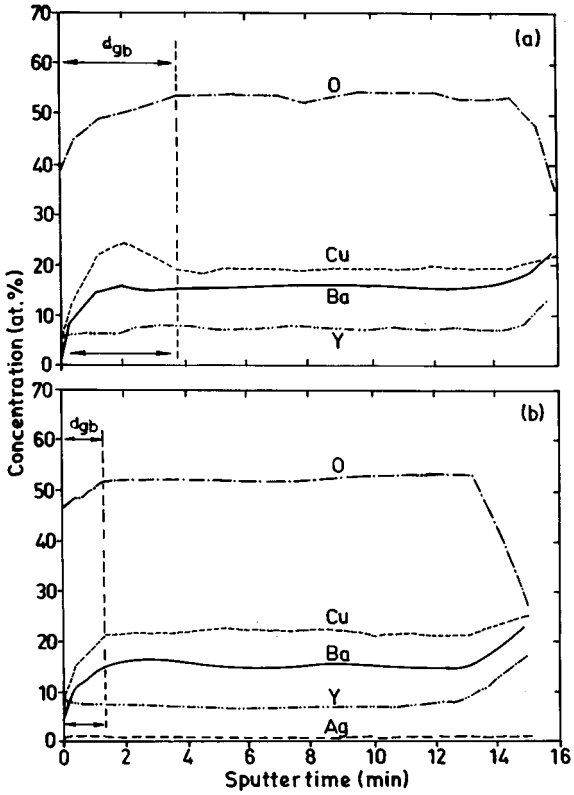

FIG. 1. Typical Auger depth profiles of (a) undoped and (b) Ag-doped $YBa_2Cu_3O_{7-\delta}$ films.

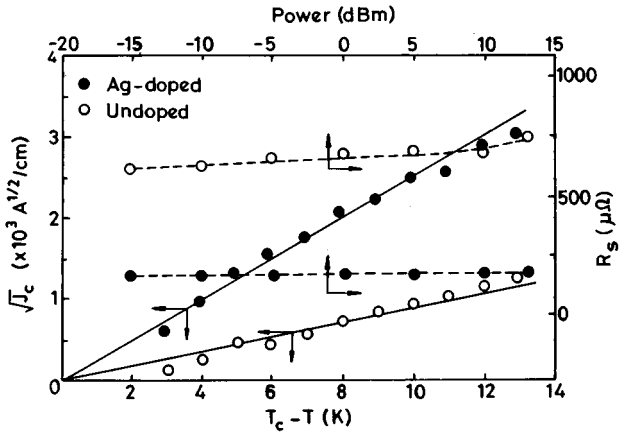

FIG. 2. Plot of $\sqrt{J_c}$ against $(T_c - T)$; and plot of R_s as a function of input power at 77 K for $YBa_2Cu_3O_{7-\delta}$ films.

slope values (see Table II) resulting in Ag-doped films indicate improved metallicity of the grain-boundary regions compared to the undoped films. Since the slope is an inverse exponential function of d_{gb}, it follows that the Ag-doped films have much smaller grain-boundary extension. This is evident from Auger depth profile results and, thus, confirming the validity of the above model. This is further supported by R_s measurements,[8] which are sensitive to the grain-boundary weak links, where a twofold decrease in R_s value is noted for the Ag-doped films (Fig. 2).

Clearly, these findings are in line with a theoretical model[26] based on the reduction in the resistive grain boundaries, R_{gb}. Assuming R_{gb} is proportional to the dimension of the grain boundary, for a general case, J_c is given by

$$J_c \propto \frac{1}{R_{gb}^{3/2}} \propto \frac{1}{d_{gb}^{3/2}}, \tag{3}$$

where the exponent value given in the equation is typical for $YBa_2Cu_3O_{7-\delta}$.[16] Now, if the sizes of the grains of undoped and Ag-doped $YBa_2Cu_3O_{7-\delta}$ are, respectively, a and ka, and the dimensions of the grain boundaries are d_{gb} and d'_{gb}, then for a unit length having ''N'' number of grains, the following relations exist:[26]

$$N(a + d_{gb}) = 1; \quad N(ka + d'_{gb}) = 1. \tag{4}$$

From Eqs. (3) and (4), the ratio of critical current densities can be obtained as

$$\frac{J'_c}{J_c} = \left(\frac{d_{gb}}{d'_{gb}}\right)^{3/2}, \tag{5}$$

where J'_c and J_c, respectively, are the critical current densities of Ag-doped and undoped $YBa_2Cu_3O_{7-\delta}$ films. From HRAES observations (Fig. 1 and Table II), the grain-boundary thicknesses (half-width) for example, the ratio of J'_c/J_c, is estimated to be 8.0 from Eq. (5), which is in good agreement with the ratio obtained (8.2) from transport measurements. Thus, there seems strong evidence that silver plays a significant role in improving the microstructure as well as effectively upgrading the interface properties, viz., narrower resistive grain boundaries of $YBa_2Cu_3O_{7-\delta}$ films and, hence, the overall J_c. The effect is comparable to those seen in the Chevrel-phase superconductors.[32]

[1] B. Dwir, M. Affronte, and D. Pavuna, Appl. Phys. Lett. **55**, 399 (1989).
[2] J. H. Miller, S. L. Holder, J. D. Hunn, and G. N. Holder, Appl. Phys. Lett. **54**, 2256 (1990).
[3] J. Jung, M. A.-K. Mohamed, S. C. Cheng, and J. P. Franck, Phys. Rev. B **42**, 6181 (1990).
[4] Y. Matsumoto, J. Hombo, Y. Yamaguchi, N. Nischida, and A. Chiba, Appl. Phys. Lett. **56**, 1585 (1990).
[5] O. Ishii, T. Konaka, M. Sato, and Y. Koshimoto, Jpn. J. Appl. Phys. 2, Lett. **29**, L1075 (1990).
[6] M. F. Davis, J. Wosik, K. Forster, S. C. Deshmukh, H. R. Rampersad, S. Shah, P. Siemsen, J. C. Wolfe, and E. J. Economou, J. Appl. Phys. **69**, 7182 (1991).
[7] R. K. Singh, D. Bhattacharya, P. Tiwari, J. Narayan, and C. B. Lee, Appl. Phys. Lett. **60**, 255 (1992).
[8] R. Pinto, P. R. Apte, C. P. D'Souza, L. C. Gupta, R. Vijayaraghavan, D. Kumar, and M. Sharon, Physica C **196**, 264 (1992).
[9] D. Kumar, M. Sharon, R. Pinto, P. R. Apte, S. P. Pai, S. C. Purandare, L. C. Gupta, and R. Vijayaraghavan, Appl. Phys. Lett. **62**, 3522 (1993).
[10] T. Clausen, M. Ejrnaes, M. Olesen, K. Hilger, J. C. Skov, P. Bodin, A. Kuhle, and I. Chorkendorff, Appl. Phys. Lett. **65**, 2350 (1994).
[11] Ch. Zhang, A. Kulpa, and A. C. D. Chaklader, Physica C **252**, 67 (1995), and references therein.
[12] C. Hart, O. Ares, J. L. Pena, P. Bartolo-Perez, V. Sosa, W. Cauich, G. A. Hirata, L. Cota-Araiza, and M. H. Farias, Appl. Phys. Lett. **67**, 2078 (1995).
[13] D. M. Kroeger, A. Choudhury, J. Brynestad, R. K. Williams, R. A. Padtett, and W. A. Coughlin, J. Appl. Phys. **64**, 331 (1988).
[14] S. E. Babcock, T. F. Kelly, P. J. Lee, J. M. Suntjens, L. A. Lavanier, and D. C. Larbalestier, Physica C **152**, 25 (1988).
[15] D. Dimos, P. Chaudhari, and J. Mannhart, Phys. Rev. B **41**, 4038 (1990).
[16] R. Gross, P. Chaudhari, M. Kawasaki, and A. Gupta, Phys. Rev. B **42**, 10 735 (1990).
[17] H. J. Sheel, M. Berkowski, and B. Chabot, Physica C **185-189**, 2095 (1991).
[18] T. Kitamura, J. G. Wen, Y. Shiohara, N. Koshizuka, I. Hirabayashi, S. Tanaka, Y. Sugawara, and Y. Ikuhara, Physica C **262**, 120 (1996).
[19] L. E. Davis, N. C. MacDonald, P. W. Palmberg, G. E. Riach, and R. E. Weber, *Hand Book of Auger Electron Spectroscopy* (Physical Electronics, Inc., Eden Prairie, MN, 1976).
[20] P. Selvam, Appl. Phys. Lett. **67**, 3650 (1995).
[21] E. W. Seibt and A. Zalar, Mater. Lett. **11**, 1 (1991); Surf. Interface Anal. **19**, 358 (1992).
[22] R. Pinto, P. R. Apte, L. C. Gupta, R. Vijayaraghavan, K. Easwar, and B. K. Sarakar, Supercond. Sci. Technol. **4**, 577 (1991).
[23] P. Selvam, J. Cors, M. Decroux, and Ø. Fischer, Appl. Phys. A **60**, 459 (1995).
[24] P. Selvam, E. W. Seibt, and M. Murugesan (unpublished results).
[25] U. De, S. Natarajan, and E. W. Seibt, Physica C **183**, 83 (1991).
[26] D. S. Misra, B. John, R. Pinto, L. S. Mombasawala, and S. B. Palmer, Physica C **248**, 276 (1995).
[27] C. W. Yuan, B. R. Zhao, Y. Z. Zhang, Y. Y. Zhao, Y. Lu, H. S. Wang, Y. H. Shi, J. Gao, and L. Li, J. Appl. Phys. **64**, 4091 (1988).
[28] L. H. Allen, P. R. Broussard, J. H. Claassen, and S. A. Wolf, Appl. Phys. Lett. **53**, 1338 (1988).
[29] G. Deutscher and K. A. Muller, Phys. Rev. Lett. **59**, 1745 (1987).
[30] P. G. Degennes, Rev. Mod. Phys. **36**, 225 (1964).
[31] J. Clarke, Phys. Rev. B **4**, 2963 (1971).
[32] P. Selvam, J. Cors, D. Cattani, M. Decroux, Ø. Fischer, and E. W. Seibt, Appl. Phys. A **61**, 615 (1995).